ARTICLE NO. 79-4059

Inhomogeneous Broadening Effects in cw Chemical Lasers

Harold Mirels*
The Aerospace Corporation, El Segundo, Calif.

The effects of inhomogeneous broadening on the performance of cw chemical lasers are investigated. A simple two-level vibrational model and a Fabry-Perot resonator are assumed. Laser performance is found to depend on the parameters $\Delta\nu_h/\Delta\nu_d$ and R, where $\Delta\nu_h$ is the homogeneous linewidth, $\Delta\nu_d$ is the Doppler line width, and R is the ratio of molecular collision rate to the excited molecule deactivation rate. Typical values are in the range $R=O(100)$ and $\Delta\nu_h/\Delta\nu_d=O(0.01\text{-}0.1)$. Analytic solutions are obtained for $[I/(1+R)]^2 \ll 1$, where I is a normalized lasing intensity. Numerical results are presented for a cw chemical laser with laminar diffusion and with a single longitudinal optical mode. The variation of differential number density ΔN and local lasing intensity I with streamwise distance and the variation of net laser output power with tuning frequency are presented. The latter exhibits a Lamb dip near line center, which is in agreement with experimental observations. Inhomogeneous broadening effects are found to become negligible for $(\Delta\nu_h/\Delta\nu_d)R \geq O(10)$. The latter parameter is approximated by the expression $(\Delta\nu_h/\Delta\nu_d)R=O[p(\text{Torr})]$ where p is the static pressure in the lasing region in Torr. Thus, in typical devices, inhomogeneous broadening effects become negligible for $p \geq O(10)$ Torr. These effects become important in single longitudinal mode lasers operating in the regime p (Torr) $\leq O(1)$ and in lasers wherein the streamwise length of the resonator is short compared with the streamwise length of the positive gain region.

Nomenclature

A,B,C = coefficients, Eq. (34)
c = speed of light in vacuum
$D(\ )$ = Dawson integral, Appendix B
FWHM = full width at half maximum
G_j,G_c = normalized gain, Eq. (20)
$g(\nu_j),g_j$ = gain per unit length at frequency ν_j, Eq. (7a)
$\bar{I}^{\pm}(\nu_j),\bar{I}_j^{\pm}$ = local lasing intensity in $\pm y$ direction
$\bar{I}$ = net local lasing intensity, $\Sigma_j \bar{I}^{\pm}(\nu_j)$
$\bar{I}_s$ = saturation intensity, $[(1+R)/2]\epsilon k_{cd}/\sigma_0$
$I^+(\nu_j),I_j$ = normalized local intensity, Eq. (20)
j = longitudinal mode number
j_f = final value of j
k = characteristic rate, s^{-1}
k_{cd} = characteristic collisional deactivation rate, s^{-1}
k_{cr} = characteristic cross relaxation rate, s^{-1}
L = separation between mirrors
$\mathcal{L}(\nu_j-\nu),\mathcal{L}_j$ = Lorentzian distribution, Eqs. (2b) and (20d)
m = one half and one for laminar and turbulent diffusion, respectively
$N_1,N_2,N_T,N_{2,\nu}$ = normalized number density per unit volume
ΔN = N_2-N_1
$n(\nu)$ = particles (moles) per unit volume in interval ν to $\nu+d\nu$
n_r = characteristic number density, $[F]_\infty$
n_T = n_1+n_2
n_2,n_1 = net particles (moles) per unit volume in upper and lower lasing levels
$\bar{P}(\zeta)$ = net output power per unit nozzle height up to station ζ
$\bar{P}_e$ = net output power per unit nozzle height
P_e = normalized net output power, Eq. (29b)
$\bar{p}(\nu),\bar{p}_0$ = Maxwellian distribution function, Eq. (5)
$p(\nu_j),p_j$ = normalized Maxwellian distribution function, Eq. (5)
p = static pressure in lasing region
R = k_{cr}/k_{cd}
R_m = mirror reflectivity
T = static temperature, K
u = flow velocity in $+x$ direction
v_y = random particle velocity in $+y$ direction
x,y = streamwise and transverse directions, respectively
x_D = characteristic diffusion distance, Eq. (17)
$y_f(x)$ = flame sheet shape, Eq. (17)
ϵ = energy per mole of photons
ζ = normalized streamwise distance, $k_{cd}x/u$
ζ_D = normalized diffusion distance, $k_{cd}x_D/u$
$\eta(\nu)$ = index of refraction, Eq. (7)
λ = wavelength
ν = frequency, s^{-1}
ν_j = lasing frequency, Eqs. (11) and (12)
$\Delta\nu_c$ = longitudinal mode separation, $c/2L$
$\Delta\nu_d$ = Doppler width (FWHM)
$\Delta\nu_h$ = homogeneous width (FWHM)
$\Delta\nu_s$ = separation between adjacent modes, Eq. (14b)
σ = cross section for simulated emission, Eq. (1)

Subscripts

0 = value at ν_0
1 = lower lasing level
2 = upper lasing level
∞ = value upstream of flame sheet
c = optical cavity value
e = value at end of lasing region
i = value at start of lasing or species
j = value corresponding to ν_j

Presented at AIAA Conference on Fluid Dynamics of High Power Lasers (classified), Cambridge, Mass., Oct. 31-Nov. 2, 1978; submitted May 22, 1978; revision received Dec. 21, 1978.

Index categories: Lasers; Reactive Flows.

*Associate Director, Aerophysics Laboratory, The Ivan A. Getting Laboratories. Fellow AIAA.

I. Introduction

THE reaction zone in cw chemical lasers (Fig. 1) is generally maintained at pressures of the order of 1 to 10

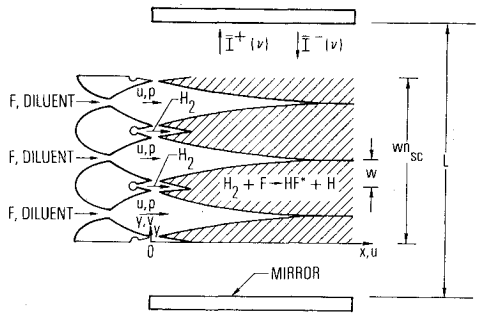

Fig. 1 cw chemical laser with F-P resonator.

Torr in order to permit fast mixing of the reactants. At these pressure levels, the spectral line shape is inhomogeneously broadened (i.e., the radiation field interacts with only a portion of the excited molecules). As a result, hole burning[1] may occur as the degree of optical saturation is increased.

In previous analytical studies of cw chemical lasers,[2,3] hole-burning effects are ignored. In these studies, it is assumed that lasing occurs at line center of the Doppler-broadened line shape and that the latter line shape is maintained in the presence of lasing. These assumptions provide for reasonable estimates of oscillator output power for cases where resonator configurations permit a large number of optical modes. However, for single-mode operation at pressure of the order of 1 to 10 Torr[4,5] and for multimode operation in relatively low-pressure devices, hole-burning effects need to be considered. These effects, in fact, have been reported in Refs. 4 and 5, where a "Lamb dip" is observed as a single-mode cw chemical laser is tuned across line center.

A comprehensive theory for inhomogeneous broadening effects in a steady-state laser oscillator has been developed by Lamb.[6] Lamb's theory is directly applicable to atomic lasing systems wherein the deactivation of excited particles (by spontaneous emission) is fast compared to the particle collision rate (i.e., the effect of collisions on the excited particle velocity distribution function is neglected). Kan and Wolga[7] extended Lamb's theory to CO_2 molecular lasers wherein the deactivation rate of excited CO_2 is slow compared to the molecular collision rate. The latter collisions tend to fill the "hole" induced by inhomogeneous broadening and need to be considered.

In the previous theories[6,7] for inhomogeneous broadening effects, flow properties do not vary temporally or spatially. The extension to cw chemical lasers is not straightforward since flow conditions in the latter are functions of streamwise distance. Hence, the present study was undertaken to evaluate the effects of inhomogeneous broadening on cw chemical laser performance. A simple two-level vibrational model similar to that used in Ref. 2 is used. A Fabry-Perot (F-P) resonator is assumed, and the variation of flow conditions with streamwise distance is considered. Discrete rotational energy states, however, are not considered.

II. Theory

The flow is considered to have a uniform velocity u in the $+x$ direction. A Fabry-Perot (F-P) resonator is aligned with its optical axis normal to the flow (Fig. 1). The total number of particles, per unit volume, in the lower and upper vibrational levels are denoted n_1 and n_2, respectively. General aspects of the interaction between the radiation field and the lasing medium are discussed. Effects of inhomogeneous broadening on the performance of a cw chemical laser are then deduced. Steady-state lasing is assumed.

A. General Considerations

In the following sections, inhomogenous broadening and the longitudinal mode structure in a F-P resonator are discussed.

Stationary Particles

Let ν_0 denote the resonant (line center) frequency for absorption or stimulated emission of radiation by particles essentially at rest. (More specifically, collisions are permitted between particles, but terms of order v_y/c compared to one are neglected.) For these particles, the gain at frequency ν can be expressed

$$g(\nu,\nu_0)=\sigma(\nu,\nu_0)\,(n_2-n_1) \tag{1}$$

where $\sigma(\nu,\nu_0)$ is the cross section for stimulated emission at ν. Equation (1) can be written in the form[8]

$$g(\nu,\nu_0)=\sigma_0[\mathcal{L}(\nu-\nu_0)](n_2-n_1) \tag{2a}$$

where $\sigma_0\equiv\sigma(\nu_0,\nu_0)$ is the cross section at ν_0 and $\mathcal{L}(\nu-\nu_0)$ is the Lorentzian (homogeneous) line shape

$$\mathcal{L}(\nu-\nu_0)\equiv\frac{\sigma(\nu,\nu_0)}{\sigma_0}=\left[1+4\left(\frac{\nu-\nu_0}{\Delta\nu_h}\right)^2\right]^{-1} \tag{2b}$$

Here, $\Delta\nu_h$ is the characteristic width (FWHM) of the homogeneous line shape and is a function of pressure (Appendix A). The broadening is due to particle collisions. The index of refraction at ν can be expressed

$$\eta(\nu,\nu_0)-1=\frac{\lambda}{2\pi}\,\frac{\nu-\nu_0}{\Delta\nu_h}\,g(\nu,\nu_0) \tag{2c}$$

which follows from the Kramers-Kronig relations.[8]

The integral of the homogeneous line shape is a constant. Thus,

$$\int_{-\infty}^{\infty}\sigma(\nu,\nu_0)\,d\nu=\frac{\pi}{2}\sigma_0\Delta\nu_h \tag{2d}$$

where $\sigma_0\Delta\nu_h$ is independent of pressure level, but $\Delta\nu_h$ and σ_0^{-1} are proportional to pressure.

Doppler Effect

The effect of random motion of the particles is considered. $\bar{I}^+(\nu)$ denotes radiation with frequency ν traveling in the $+y$ direction, and v_y, the random particle velocity, in $+y$ direction (Fig. 1). Because of the Doppler effect, the frequency ν, which will be resonant with particles with a velocity v_y is $\nu=\nu_0/[1-(v_y/c)]$ which, for the realistic assumption $v_y/c\ll 1$, becomes

$$\nu=\nu_0[1+(v_y/c)] \tag{3a}$$

Conversely, the particle velocity v_y, which will result in resonance with $\bar{I}^+(\nu)$, is

$$v_y/c=(\nu/\nu_0)-1 \tag{3b}$$

In the absence of radiation, the particles in the upper and lower vibrational levels can be assumed to have a Maxwellian velocity distribution. The number of particles resonant with frequencies in the range ν to $\nu+d\nu$ is then $n(\nu)\,d\nu$, where[8]

$$\frac{n(\nu)}{n}=\frac{1}{\Delta\nu_d}\left(\frac{4\ell n2}{\pi}\right)^{1/2}\exp\left[-(4\ell n2)\left(\frac{\nu-\nu_0}{\Delta\nu_d}\right)^2\right] \tag{4}$$

Here, $\Delta\nu_d$ is the characteristic (Doppler) width (FWHM) of the Maxwellian distribution [Eq. (A1)]. For later use, the notations

$$\bar{p}(\nu)\equiv n(\nu)/n,\quad p(\nu)\equiv\bar{p}(\nu)/\bar{p}_0 \tag{5a}$$

and

$$\tilde{p}_0 \equiv \tilde{p}(\nu_0) = [(4\ell n 2)/\pi]^{1/2}/\Delta\nu_d \tag{5b}$$

are introduced. Note that

$$\int_{-\infty}^{\infty} \tilde{p}(\nu)\,d\nu = \tilde{p}_0 \int_{-\infty}^{\infty} p(\nu)\,d\nu = 1 \tag{5c}$$

Upon reflection from a lossless mirror, $\tilde{I}^+(\nu)$ will be converted to $\tilde{I}^-(\nu)$, which, as a result of the Dopper effect, interacts with particles with velocity $v_y/c = -[(\nu/\nu_0) - 1]$. Thus, $\tilde{I}^{\pm}(\nu)$ interact with the velocity groups $v_y/c = \pm[(\nu/\nu_0) - 1]$, respectively. Note also that $\tilde{I}^-(\nu)$ and $\tilde{I}^+(2\nu_0 - \nu)$ interact with the same particles. This equivalence is used in the subsequent treatment of an F-P resonator. In particular, particle groups are identified by the resonant frequency associated with the wave $\tilde{I}^+(\nu)$. Also, integration over all population groups is accomplished by integration with respect to ν in the interval $-\infty < \nu < \infty$ rather than by integration with respect to v_y in the interval $-\infty < v_y < \infty$.

Inhomogeneous Broadening

Under lasing conditions, the particle distribution function is perturbed from the Maxwellian, and more general distributions need to be considered. Thus, from Eq. (2), the gain and refractive index at ν' resulting from particles that are resonant with radiation in the range ν to $\nu + d\nu$ can be expressed (Fig. 2)

$$dg(\nu') = \sigma_0 \mathcal{L}(\nu' - \nu)[n_2(\nu) - n_1(\nu)]\,d\nu \tag{6a}$$

$$d[\eta(\nu') - 1] = \frac{\sigma_0 c}{2\pi\nu_0} \frac{\nu' - \nu}{\Delta\nu_h} \mathcal{L}(\nu' - \nu)[n_2(\nu) - n_1(\nu)]\,d\nu \tag{6b}$$

The net gain and refractive index at ν' is then found by integration over all particle groups. The result is

$$g(\nu') = \sigma_0 \int_{-\infty}^{\infty} \mathcal{L}(\nu' - \nu)[n_2(\nu) - n_1(\nu)]\,d\nu \tag{7a}$$

$$\eta(\nu') - 1 = \frac{\lambda\sigma_0}{2\pi} \int_{-\infty}^{\infty} \frac{\nu' - \nu}{\Delta\nu_h} \mathcal{L}(\nu' - \nu)[n_2(\nu) - n_1(\nu)]\,d\nu \tag{7b}$$

Equations (7) define the gain and refractive index of an inhomogeneously broadened medium. The evaluation of Eqs. (7) for a chemical laser medium is the subject of the present study. Amplification of $\tilde{I}^{\pm}(\nu')$ is found from

$$\frac{d\tilde{I}^{\pm}(\nu')}{dy} = \pm g(\nu')\tilde{I}^{\pm}(\nu') \tag{8}$$

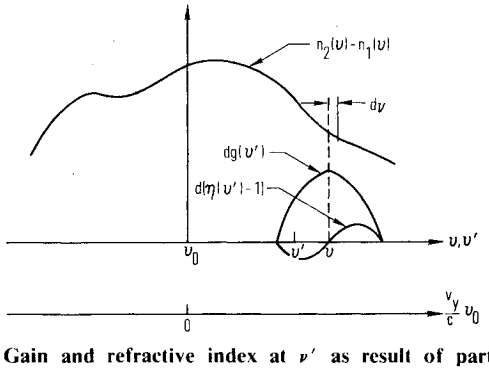

Fig. 2 Gain and refractive index at ν' as result of particles in frequency interval ν to $\nu + d\nu$.

For a nonlasing medium, Eq. (4) is applicable, and Eq. (7) becomes

$$\frac{g(\nu')}{(\pi/2)[\sigma_0\tilde{p}_0\Delta\nu_h(n_2 - n_1)]} = \frac{2}{\pi}\int_{-\infty}^{\infty} p(\nu)\mathcal{L}(\nu' - \nu)\frac{d\nu}{\Delta\nu_h} \tag{9a}$$

$$\frac{(4\pi/\lambda)[\eta(\nu') - 1]}{(\pi/2)[\sigma_0\tilde{p}_0\Delta\nu_h(n_2 - n_1)]} = \frac{4}{\pi}\int_{-\infty}^{\infty} \frac{\nu' - \nu}{\Delta\nu_h} p(\nu)\mathcal{L}(\nu' - \nu)\frac{d\nu}{\Delta\nu_h} \tag{9b}$$

The right-hand sides (RHS) of Eqs. (9a) and (9b) equal the real and imaginary part of a complex error function.[9,10] For $(\tilde{p}_0\Delta\nu_h)^2 \ll 1$, these quantities can be deduced from Eqs. (B1d) and (B1e) with $\phi_j = 1$ therein.

Resonator Modes

An F-P resonator can support longitudinal modes centered at frequencies $\nu = Nc/2L$, where N is an integer and L is the separation between mirrors. The longitudinal mode separation is then $\Delta\nu_c = c/2L$. A typical longitudinal mode distribution is illustrated by the solid lines in Fig. 3. The frequency width of each mode can be assumed to be small compared to $\Delta\nu_h$.

A convenient notation for dealing with the interaction between the resonator modes and the gain medium is now introduced. Without loss of generality it can be assumed that one longitudinal mode, centered at ν_1, is located in the interval

$$\nu_0 < \nu_1 < \nu_0 + (\Delta\nu_c/2) \tag{10}$$

The central frequency of the longitudinal modes can be expressed in the form

$$\nu_j = \nu_1 + (j-1)(\Delta\nu_c/2) \quad j = 1,3,5,\ldots \tag{11a}$$

$$= \nu_1 + j(\Delta\nu_c/2) \quad j = -2,-4,-6,\ldots \tag{11b}$$

These frequencies are denoted by solid lines in Fig. 3. The radiation $\tilde{I}^+(\nu_j)$ interacts with particles characterized by the frequency $\nu = \nu_j$ in Fig. 3. The interaction results in the "holes" indicated therein. As previously noted, the interaction of the reflected radiation $\tilde{I}^-(\nu_j)$ with the lasing medium is equivalent to the interaction of $\tilde{I}^+(2\nu_0 - \nu_j)$ with this medium. An equivalent $I^+(\nu_j)$ radiation field with frequencies defined by

$$\nu_j = 2\nu_0 - \nu_1 + j(\Delta\nu_c/2) \quad j = 2,4,6,\ldots \tag{12a}$$

$$= 2\nu_0 - \nu_1 + (j+1)(\Delta\nu_c/2) \quad j = -1,-3,-5,\ldots \tag{12b}$$

is considered. The latter are indicated by the dashed lines in Fig. 3. These lines are the mirror image of the solid lines,

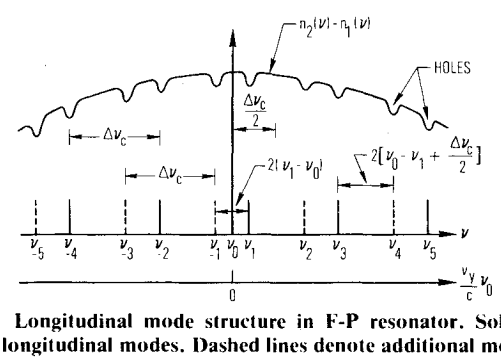

Fig. 3 Longitudinal mode structure in F-P resonator. Solid lines denote longitudinal modes. Dashed lines denote additional modes for equivalent resonator with radiation in $+y$ direction only.

about ν_0, and also have a separation $\Delta\nu_c$. The results of the present approach are identical with those obtained from an F-P resonator with both $\bar{I}^+$ and $\bar{I}^-$ radiation.

A further simplification can be introduced. Because of the symmetry about ν_0, only lasing frequencies in the interval $\nu_j > \nu_0$ need to be considered. These are given by Eqs. (11a) and (12a). In particular, $j = 1,2,3,\ldots j_f$ is considered, where j_f is the value of j for the last (final) lasing transition in the interval $\nu_j > \nu_0$. The total number of lasing transitions is $2j_f$. the sum of a quantity $(\,)_j$ over all j is then

$$\sum_j (\,)_j \equiv \sum_{j=\pm 1}^{j=\pm j_f} (\,)_j = 2\sum_{j=1}^{j_f} (\,)_j \tag{13}$$

When lasing transitions are separated by a frequency difference of order $\Delta\nu_h$, they compete for the same particles. Later, $\Delta\nu_h \ll \Delta\nu_c$ is assumed so that, at most, only two radiation fields can compete. Two cases can be distinguished. When $0 < \nu_1 - \nu_0 < (\Delta\nu_c/4)$, the separation between adjacent modes $\Delta\nu_s$ is (Fig. 3)

$$\Delta\nu_s = 2(\nu_1 - \nu_0) \tag{14a}$$

If $\Delta\nu_s/\Delta\nu_h = O(1)$, competition will occur between ν_{-1} and ν_1, ν_2 and ν_3, ν_4 and $\nu_5, \ldots$. Here, j_f is odd. When $(\Delta\nu_c/4) < \nu_1 - \nu_0 < (\Delta\nu_c/2)$, the separation between adjacent modes is (Fig. 3)

$$\Delta\nu_s = 2[\nu_0 - \nu_1 + (\Delta\nu_c/2)] \tag{14b}$$

If $\Delta\nu_s/\Delta\nu_h = O(1)$, competition occurs between ν_1 and ν_2, ν_3 and $\nu_4, \ldots$. Here, j_f is even. When $\Delta\nu_s \gg \Delta\nu_h$, no mode competition occurs.

The open interval is used in Eq. (10) to avoid the degenerate case where two lasing transitions overlap in Fig. 3 (i.e., $\Delta\nu_s = 0$). This case is treated herein by consideration of the limit $\Delta\nu_s \to 0$.

Resonator Boundary Condition

Diffraction effects are neglected, and it is assumed that each mirror of the F-P resonator has the same reflectivity R_m. Later, it is assumed that there are n_{sc} semichannels, each of width w, and that the lateral width of the gain region in each semichannel is $y_f(x)$ (Fig. 4). Under steady-state lasing conditions, the net gain per pass equals the net loss per pass at each streamwise station where lasing occurs. For these conditions, the local gain is defined by

$$g_j = \frac{-\ell n R_m}{n_{sc} y_f(x)} \equiv g_c \tag{15}$$

where $g_j \equiv g(\nu_j)$.

B. General Solution

The equations that define the effects of gain saturation on the performance of a Doppler-broadened cw chemical laser are deduced. A premixed flow is first discussed. Effects of diffusion then are introduced.

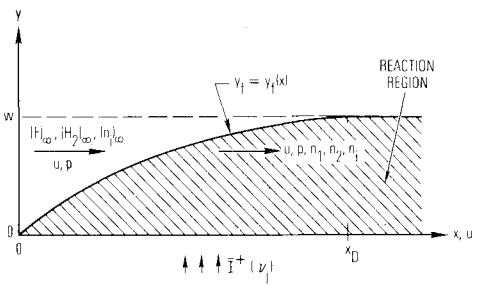

Fig. 4 Simplified model of cw chemical laser. A single semichannel is shown.

Premixed Laser

At sufficiently low pressures, the rate of diffusion can be considered fast, relative to the rate of chemical reactions in a cw chemical laser. For these conditions, the reactants can be considered to be premixed and to start reacting at $x = 0$. Fluid properties are a function only of streamwise distance x. The rate of change of $n_2(\nu)$ and $n_1(\nu)$ with x can then be expressed

$$u\frac{dn_2(\nu)}{dx} = \bar{p}(\nu)u\frac{dn_T}{dx} - k_{cd}n_2(\nu) + k_{cr}[\bar{p}(\nu)n_2 - n_2(\nu)] - \frac{n_2(\nu) - n_1(\nu)}{\epsilon}\sum_j \bar{I}_j\sigma(\nu_j,\nu) \tag{16a}$$

$$u\frac{dn_1(\nu)}{dx} = 0 + k_{cd}n_2(\nu) + k_{cr}[\bar{p}(\nu)n_1 - n_1(\nu)] + \frac{n_2(\nu) - n_1(\nu)}{\epsilon}\sum_j \bar{I}_j\sigma(\nu_j,\nu) \tag{16b}$$

where $\bar{I}_j \equiv \bar{I}^+(\nu_j)$ and $n_T = n_1 + n_2$. The terms on the RHS of Eq. (16a) have the following interpretation. In the first term, the chemical pumping reaction (which is considered known)[2] is assumed to create only n_2 particles, which initially have a Maxwellian velocity distribution. The second term represents the loss resulting from collisional deactivation. The rate coefficient k_{cd} is assumed to be independent of ν. The third term represents the creation of $n_2(\nu)$ as a result of cross relaxation. The latter is assumed equal to the product of a cross relaxation rate coefficient k_{cr} with the difference between the equilibrium Maxwellian value and the local value of $n_2(\nu)$. This model is similar to that used in Ref. 11, in which a steady-state four-level amplifier was treated. The last term represents the loss of $n_2(\nu)$ as a result of stimulated emission centered at ν_j. This term is deduced from Eq. (8) and is nonzero only when $\nu - \nu_j \leq O(\Delta\nu_h)$. When n is in moles per unit volume, the quantity ϵ equals the energy per mole of photons. The terms on the RHS of Eq. (16b) can be deduced from the preceding discussion.

Diffusion Effect

A simplified diffusion model is adopted (Fig. 4). It is assumed[2,12] that the chemical reactants are premixed, but do not start to react until they enter the reaction zone bounded by $y_f = y_f(x)$. Laminar and turbulent mixing are modeled by

$$(y_f/w) = (x/x_D)^m \tag{17}$$

where $m = \frac{1}{2}$ and 1 for laminar and turbulent flow, respectively. Here, w is the semiwidth of a single oxidizer (F) nozzle, and x_D is the distance at which the reaction zone reaches the nozzle centerline. The latter is a measure of diffusion rate and is assumed to occur downstream of the lasing region.

When mean rates are used, fluid properties within the reaction zone may be assumed to vary only with x. For species n_i, the variations can be expressed[12,13]

$$\frac{u}{y_f}\frac{d[(n_i - (n_i)_\infty]y_f}{dx} = w_i \tag{18}$$

where $(n_i)_\infty$ is the number density upstream of the flame sheet, and w_i is the volumetric production rate of n_i resulting from chemical, collisional, and radiative processes. Note that

$[n_2(\nu)]_\infty = 0$; Eq. (16a) becomes

$$\frac{u}{y_f}\frac{\mathrm{d}[n_2(\nu)y_f]}{\mathrm{d}x} = \frac{u\bar{p}(\nu)}{y_f}\frac{\mathrm{d}(n_T y_f)}{\mathrm{d}x} - k_{cd}n_2(\nu) + k_{cr}[\bar{p}(\nu)n_2 - n_2(\nu)] - \frac{n_2(\nu)-n_1(\nu)}{\epsilon}\sum_j \sigma(\nu_j,\nu)\bar{I}_j \quad (19)$$

A similar equation is deduced for $n_1(\nu)$. The following normalized unit order variables are introduced

$$N_2 = \frac{n_2 y_f}{n_r w} \qquad N_{2\nu} = \frac{n_2(\nu)y_f}{n_r w \bar{p}_0} \quad (20a)$$

$$N_T = \frac{n_T y_f}{n_r w} \qquad N_{1\nu} = \frac{n_1(\nu)y_f}{n_r w \bar{p}_0} \quad (20b)$$

$$\zeta = \frac{k_{cd}x}{u} \qquad \zeta_D = \frac{k_{cd}x_D}{u} \quad (20c)$$

$$R = \frac{k_{cr}}{k_{cd}} \qquad \mathfrak{L}_j = \frac{\sigma(\nu_j,\nu)}{\sigma_0} \quad (20d)$$

$$I_j = \frac{\sigma_0 \bar{I}_j}{\epsilon k_{cd}} \qquad I = \sum_j I_j = 2\sum_{j=1}^{jf} I_j \quad (20e)$$

$$G_j = \frac{g_j y_f}{\sigma_0 n_r \Delta\nu_h \bar{p}_0 w} \qquad G_c = \frac{-\ell n R_m}{\sigma_0 n_r \Delta\nu_h \bar{p}_0 w n_{sc}} \quad (20f)$$

Here, n_r is a characteristic number density, which for a chemical laser is taken to be equal to the F atom concentration upstream of the flame sheet ($n_r \equiv [F]_\infty$). The local lasing intensity $\bar{I}_j$ is normalized herein by $\epsilon k_{cd}/\sigma_0$. Thus, the quantity I_j is the ratio of the stimulated emission rate to the rate of collisional deactivation of particles in the frequency interval $\Delta\nu_h$ about ν_j. An alternate normalization, not used herein, is $I \equiv \bar{I}/\bar{I}_s$ where $\bar{I}_s \equiv [(1+R)/2]\epsilon k_{cd}/\sigma_0$ is the appropriate measure of saturation intensity in the present model [e.g., Eq. (28)]. Thus, $2I/(1+R)$ is a measure of degree of saturation in the present model. The normalized gain at ν_j is obtained from

$$G_j = \int_{-\infty}^{\infty} \mathfrak{L}(\nu-\nu_j)(N_{2\nu}-N_{1\nu})\frac{\mathrm{d}\nu}{\Delta\nu_h} \quad (21a)$$

In the absence of lasing, $N_{2\nu}-N_{1\nu} = p(\nu)(N_2-N_1)$, and

$$G_j = (N_2-N_1)\int_{-\infty}^{\infty} p(\nu)\mathfrak{L}(\nu-\nu_j)\frac{\mathrm{d}\nu}{\Delta\nu_h} \quad (21b)$$

When $\Delta\nu_h/\Delta\nu_d \ll 1$, Eq. (21b) becomes

$$G_j = \left(\frac{\pi}{2}\right)p_j(N_2-N_1)\left[1+0\left(\frac{\Delta\nu_h}{\Delta\nu_d}\right)\right] \quad (21c)$$

where $p_j \equiv p(\nu_j)$. Threshold is reached when $G_j = G_c$.

Substitution of Eq. (20) into Eq. (19) and the equivalent expression for $n_1(\nu)$ yields

$$\frac{\mathrm{d}N_{2\nu}}{\mathrm{d}\zeta} = p(\nu)\frac{\mathrm{d}N_T}{\mathrm{d}\zeta} - N_{2\nu} + R[p(\nu)N_2 - N_{2\nu}] - (N_{2\nu}-N_{1\nu})\sum_j \mathfrak{L}_j I_j \quad (22a)$$

$$\frac{\mathrm{d}N_{1\nu}}{\mathrm{d}\zeta} = N_{2\nu} + R[p(\nu)N_1 - N_{1\nu}] + (N_{2\nu}-N_{1\nu})\sum_j \mathfrak{L}_j I_j \quad (22b)$$

where $\mathrm{d}N_T/\mathrm{d}\zeta$ is known. Integrals of Eq. (22) form the basis of the present study. Addition of Eqs. (22a) and (22b) and integration with respect to ζ and ν yields, respectively

$$N_{2\nu} + N_{1\nu} = p(\nu)N_T \quad (23a)$$

and

$$N_2 + N_1 = N_T \quad (23b)$$

The fact that Eq. (23a) is independent of R is somewhat surprising and indicates that the increase in $N_{2\nu}$, as a result of cross relaxation, is offset by an equivalent loss in $N_{1\nu}$. Equation (23b) is consistent with the definition of N_T. Subtraction of Eq. (22b) from Eq. (22a) and integration with respect to ν yields, respectively,

$$\frac{\mathrm{d}(N_{2\nu}-N_{1\nu})}{\mathrm{d}\zeta} + (1+R)(N_{2\nu}-N_{1\nu}) = p(\nu)\left[\frac{\mathrm{d}N_T}{\mathrm{d}\zeta} - N_T + R(N_2-N_1)\right] - 2(N_{2\nu}-N_{1\nu})\sum_j \mathfrak{L}_j I_j \quad (24a)$$

and

$$\frac{\mathrm{d}(N_2-N_1)}{d\zeta} + (N_2-N_1) = \frac{\mathrm{d}N_T}{\mathrm{d}\zeta} - N_T - 2(\bar{p}_0\Delta\nu_h)G_c I \quad (24b)$$

The last term on the right-hand side of Eq. (24b) follows because $G_j = G_c$ when $I_j \neq 0$. The zero power solution $I = 0$ of Eq. (24b) is

$$N_2 - N_1 = 2e^{-\zeta}\int_0^{\zeta} e^{\zeta_0}\left(\frac{\mathrm{d}N_T}{\mathrm{d}\zeta_0}\right)\mathrm{d}\zeta_0 - N_T \quad (25)$$

which, together with the relation $N_1 + N_2 = N_T$, defines N_1 and N_2. In order to evaluate Eq. (24) for $I \neq 0$, note that for $I_j \neq 0$ (i.e., $G_j = G_c$),

$$\frac{\mathrm{d}G_j}{\mathrm{d}\zeta} = \int_{-\infty}^{\infty} \mathfrak{L}(\nu-\nu_j)\frac{\mathrm{d}(N_{2\nu}-N_{1\nu})}{\mathrm{d}\zeta}\frac{\mathrm{d}\nu}{\Delta\nu_h} = 0 \quad (26a)$$

Equation (26a) is satisfied by $\mathrm{d}(N_{2\nu}-N_{1\nu})/\mathrm{d}\zeta = 0$, which is a sufficient, but not a necessary, condition, suggesting that for $I_j \neq 0$

$$\frac{\mathrm{d}(N_{2\nu}-N_{1\nu})/\mathrm{d}\zeta}{p(\nu)[(\mathrm{d}N_T/\mathrm{d}\zeta) - N_T + R(N_2-N_1)]} \ll 1 \quad (26b)$$

be assumed† in Eq. (24a). The latter becomes, with j' used as the summation index,

$$N_{2\nu} - N_{1\nu} = \frac{p(\nu)[(\mathrm{d}N_T/\mathrm{d}\zeta) - N_T + R(N_2-N_1)]}{1+R+2\sum_{j'}\mathfrak{L}(\nu-\nu_{j'})I_{j'}} \quad (27)$$

Multiplication by $\mathfrak{L}(\nu-\nu_j)\mathrm{d}\nu/\Delta\nu_h$ and integration yields, for $I_j \neq 0$,

$$\frac{1+R}{p_j}\frac{G_c}{(\mathrm{d}N_T/\mathrm{d}\zeta) - N_T + R(N_2-N_1)} = \frac{1}{p_j}\int_{-\infty}^{\infty}\frac{p(\nu)\mathfrak{L}(\nu-\nu_j)\mathrm{d}\nu/\Delta\nu_h}{1+[2/(1+R)]\sum_{j'}\mathfrak{L}(\nu-\nu_{j'})I_{j'}} \quad (28)$$

†The validity of Eq. (26b) for cw chemical lasers can be further supported by noting that all quantities in this equation are of order one except for R which can be considered large (Appendix A). The validity of Eq. (26b) for moderate values of R, however, requires further study.

Equation (28) provides j_f implicit relations between I_j and N_2-N_1, which can be used to integrate Eq. (24b). This integration provides N_2-N_1 and I_j as functions of ζ, and all other laser properties of interest can be readily deduced. For example, the power emitted in the interval $0\le x_0\le x$ by a laser of unit height is found from

$$\bar{P}(x)=n_{sc}\int_0^x y_f g_c \bar{I}\,dx_0 \tag{29a}$$

In nondimensional variables, Eq. (29a) becomes

$$P(\zeta)\equiv\frac{\bar{P}(x)}{\epsilon u n_r w n_{sc}}=\bar{p}_0\Delta\nu_h\int_0^\zeta G_c I\,d\zeta_0 \tag{29b}$$

The streamwise station at which lasing ends ($I=0$) is denoted ζ_e and the corresponding laser net output power is denoted P_e. Similarly, the refractive index in the lasing region can be obtained from

$$\frac{1+R}{p_j}\frac{2\pi}{\lambda}\frac{[\eta(\nu_j)-1]y_f/w}{\sigma_0 n_r\bar{p}_0\Delta\nu_h}\left[\frac{dN_T}{d\zeta}-N_T+R(N_2-N_1)\right]^{-1}$$
$$=\frac{1}{p_j}\int_{-\infty}^{\infty}\frac{\nu_j-\nu}{\Delta\nu_h}\frac{p(\nu)\,\mathcal{L}(\nu_j-\nu)\,d\nu/\Delta\nu_h}{1+[2/(1+R)]\sum_{j'}\mathcal{L}(\nu_{j'}-\nu)I_{j'}} \tag{29c}$$

For cases with no mode competition, $\Delta\nu_s\gg\Delta\nu_h$, the summation in Eqs. (28) and (29c) contains only a single term and the integrals can be evaluated in closed form (Appendix B).

The solution of the system of equations defined by Eqs. (24b) and (28) generally requires numerical integration. Closed-form solutions can be obtained in limiting cases, however, and these are discussed in the next section.

C. Limiting Cases

The assumptions $\Delta\nu_h\ll\Delta\nu_c$ and $\Delta\nu_h\ll\Delta\nu_d$ are introduced in order to simplify the integration of Eq. (28). The limiting cases $[2I_j/(1+R)]^2\ll 1$ and $\Delta\nu_s\ll\Delta\nu_h$ are then discussed.

When $\Delta\nu_h\ll\Delta\nu_c$, at most, two radiation fields compete for the same particles. These fields are denoted $j'=j$ and $j'=j+1$ in Eq. (28). From the assumption $\Delta\nu_h\ll\Delta\nu_d$, it follows that $p(\nu)\doteq p_j$, and, when two fields compete, $I_j\doteq I_{j+1}$. The right-hand side (RHS) of Eq. (28) then becomes

$$\text{RHS}=\int_{-\infty}^{\infty}\frac{\mathcal{L}(\nu-\nu_j)\,d\nu/\Delta\nu_h}{1+[2/(1+R)]I_j[\mathcal{L}(\nu-\nu_j)+\mathcal{L}(\nu-\nu_{j+1})]} \tag{30}$$

where, from Eq. (14), $\nu_{j+1}-\nu_j\equiv\Delta\nu_s$. Two limiting cases are treated, i.e., $[2I_j/(1+R)]^2\ll 1$ and $\Delta\nu_s\ll\Delta\nu_h$.

Case $[2I_j/(1+R)]^2\ll 1$

The present case corresponds to weak saturation. With the expansion $(1+\epsilon)^{-1}=1-\epsilon+0(\epsilon^2)$ and the use of Appendix B:

$$\text{RHS}=\frac{\pi}{2}\left\{1-\frac{I_j}{1+R}\left[1+\mathcal{L}\left(\frac{\Delta\nu_s}{2}\right)\right]+0\left(\frac{I_j}{1+R}\right)^2\right\} \tag{31}$$

Substitution into Eq. (28), taking the reciprocal of both sides, and solving for I_j yields,

$$\frac{2I_j}{1+R}=\frac{2}{1+\mathcal{L}(\Delta\nu_s/2)}\left[\frac{\pi}{2}\frac{[(dN_T/d\zeta)-N_T+R(N_2-N_1)]p_j}{(1+R)G_c}-1\right] \tag{32}$$

The total intensity is, from Eq. (13),

$$\frac{2I}{1+R}=\frac{4}{1+\mathcal{L}(\Delta\nu_s/2)}\left[\frac{\pi}{2}\frac{[(dN_T/d\zeta)-N_T+R(N_2-N_1)]}{(1+R)G_c}\times\sum_{j=1}^{j_f}p_j-j_f\right] \tag{33}$$

The present solution is self-consistent when the square of the right-hand side of Eq. (32) is small relative to one.

A closed-form solution of Eq. (24b) can be obtained in the present limit. With the constants

$$A=1+\frac{2\pi R(\bar{p}_0\Delta\nu_h)\sum_{j=1}^{j_f}p_j}{1+\mathcal{L}(\Delta\nu_s/2)} \tag{34a}$$

$$B=1-\frac{A-1}{R} \tag{34b}$$

$$C=\frac{4j_f(1+R)G_c\bar{p}_0\Delta\nu_h}{1+\mathcal{L}(\Delta\nu_s/2)} \tag{34c}$$

introduced, Eqs. (33) and (24b) become

$$2(\bar{p}_0\Delta\nu_h)G_cI=\frac{A-1}{R}\left(\frac{dN_T}{d\zeta}-N_T\right)+(A-1)(N_2-N_1)-C \tag{35}$$

$$\frac{d(N_2-N_1)}{d\zeta}+A(N_2-N_1)=B\left(\frac{dN_T}{d\zeta}-N_T\right)+C \tag{36}$$

Equation (36) applies to the nonlasing as well as the lasing regime. Lasing is initiated on a given transition ν_j at the station, where G_j first becomes equal to G_c [Eq. (21c)]. At small ζ, N_2-N_1 is small and threshold is not reached. Here, $A=B=1$, $C=0$, and Eq. (36) agrees with Eq. (24b), with $I=0$. Lasing is first achieved, by definition, on the ν_1 transition. The quantites A, B, and C are then re-evaluated with $j_f=1$ and remain constant until the second transition is initiated. Thus, A, B, and C are piecewise uniform in intervals $\zeta_i<\zeta<\zeta_{i+1}$, which are defined by the initiation or termination of lasing transitions. The piecewise integral of Eq. (36) for the interval ζ_i to ζ_{i+1}, is

$$\frac{A}{B}(N_2-N_1)e^{A\zeta_0}\Big]_{\zeta_i}^{\zeta}=(A+1)\int_{\zeta_i}^{\zeta}e^{A\zeta_0}\frac{dN_T}{d\zeta_0}d\zeta_0+\left[\left(\frac{C}{B}-N_T\right)e^{A\zeta_0}\right]_{\zeta_i}^{\zeta} \tag{37}$$

The net power emitted in this interval is from Eqs. (29) and (35)

$$\frac{2R}{A-1}P(\zeta_0)\Big]_{\zeta_i}^{\zeta}=\left(N_T-\frac{CR}{A-1}\zeta_0\right)_{\zeta_i}^{\zeta}+\int_{\zeta_i}^{\zeta}[R(N_2-N_1)-N_T]d\zeta_0 \tag{38}$$

where N_2-N_1 is obtained from Eq. (38). Equations (23, 35, 37, and 38) define the performance of a chemical laser, provided N_T is known.

Case $\Delta\nu_s \ll \Delta\nu_h$

In this case, the competing lasing modes have nearly the same frequency. Thus, $\mathcal{L}(\nu-\nu_{j+1}) = \mathcal{L}(\nu-\nu_j)[1+0(\Delta\nu_s/\Delta\nu_h)]$.

Integration of Eq. (28) and the use of Appendix B yields

$$\frac{2I_j}{1+R} = \frac{1}{2}\left\{\left[\frac{\pi}{2}\frac{[(dN_T/d\zeta)-N_T+R(N_2-N_1)]p_j}{(1+R)G_c}\right]^2 - 1\right\} \quad (39)$$

and

$$\frac{2I}{1+R} = \left[\frac{\pi}{2}\frac{(dN_T/d\zeta)-N_T+R(N_2-N_1)}{(1+R)G_c}\right]^2 \sum_{j=1}^{j_f} p_j^2 - j_f \quad (40)$$

In the limit $[I_j/(1+R)]^2 \ll 1$, $\Delta\nu_s \to 0$ Eqs. (32) and (39) are in agreement, as expected. Substitution of Eq. (40) into Eq. (24b) yields a first-order nonlinear equation that requires numerical integration.

D. Pumping Rate

An expression for N_T is needed. A useful limiting case is to assume that the chemical reaction that creates excited species (i.e., the pumping reaction) is fast relative to the diffusion rate. In the present model,[2,12] this reaction is equivalent to the assumption that n_r (i.e., $[F]_\infty$) is converted to n_2 (i.e., [HF*]) at the instant that the n_r particles enter the reaction zone bounded by y_f. It follows that

$$N_T = \frac{y_f}{w} = \left(\frac{\zeta}{\zeta_D}\right)^m \quad (41)$$

where $m = \frac{1}{2}$ and 1 for laminar and turbulent flows, respectively.

E. Laminar Diffusion

Laminar diffusion is considered and analytic solutions deduced for the zero-power case and for $[2I_j/(1+R)]^2 \ll 1$.

Zero Power

Substitution of Eq. (41), with $m = \frac{1}{2}$, into Eq. (25) yields

$$\zeta_D^{1/2}(N_2-N_1) = 2D(\zeta^{1/2}) - \zeta^{1/2} \quad (42)$$

where $D(\ )$ is the Dawson integral. Since gain saturation effects do not enter into the zero-power solution, the present results are identical to those of Ref. 2. The population inversion has a maximum $\zeta_D^{1/2}(N_2-N_1) = 0.3528$ at $\zeta = 0.3051$. The inversion is zero at $\zeta = 1.1301$. Further results are given in Ref. 2. The station at which lasing is initiated can be determined from Eqs. (42) and (21). Thus, for $j=1$, lasing is initiated at the station ζ_i, which is defined by

$$\frac{2}{\pi}\frac{\zeta_D^{1/2}G_c}{p_1} = \zeta_D^{1/2}(N_2-N_1)_i = 2D(\zeta_i^{1/2}) - \zeta_i^{1/2} \quad (43)$$

from which, it follows that $0 < \zeta_i < 0.3051$. Values of G_c that permit lasing are defined by $2\zeta_D^{1/2}G_c/\pi p_1 < 0.3528$.

Case $[2I_j/(1+R)]^2 \ll 1$

Substitution of Eq. (41) into Eq. (37) yields

$$\frac{A}{B}\zeta_D^{1/2}\left[(N_2-N_1)e^{A\zeta_0}\right]_{\zeta_i}^{\zeta}$$

$$= \left(e^{A\zeta_0}\left\{\frac{A+1}{A^{1/2}}D[(A\zeta_0)^{1/2}] - \zeta_0^{1/2} + \frac{C}{B}\zeta_D^{1/2}\right\}\right)_{\zeta_i}^{\zeta} \quad (44a)$$

$$\frac{A}{B}\int_{\zeta_i}^{\zeta}\zeta_D^{1/2}(N_2-N_1)\,d\zeta_0 = \left(\frac{A+1}{A}\left\{\zeta_0^{1/2} - \frac{D[(A\zeta_0)^{1/2}]}{A^{1/2}}\right\}\right.$$

$$\left. - \frac{2}{3}\zeta_0^{3/2} + \frac{C}{B}\zeta_D^{1/2}\zeta_0\right)_{\zeta_i}^{\zeta} + \left[\frac{e^{-A(\zeta-\zeta_i)}-1}{A}\right]$$

$$\times\left\{\frac{A+1}{A^{1/2}}D[(A\zeta_i)^{1/2}] - \zeta_i^{1/2} + \frac{C}{B}\zeta_D^{1/2} - \frac{A}{B}\zeta_D^{1/2}(N_2-N_1)_i\right\} \quad (44b)$$

Substitution of these expressions into Eqs. (35) and (38) yields explicit expressions for the local lasing intensity and net output power. It is of interest to evaluate the lasing intensity at the station where lasing is initiated. Substitution of Eq. (35) [note Eq. (34)] yields (with $p_j = p_1$ and $\zeta = \zeta_i$)

$$\zeta_D^{1/2}G_cI_i = \frac{\pi p_1}{1+\mathcal{L}(\Delta\nu_s/2)}\left\{\frac{1}{2\zeta_i^{1/2}} - 2D(\zeta_i^{1/2})\right\} \quad (45)$$

For ζ_i near 0.3051, I is small and the assumption $[I/(1+R)]^2 \ll 1$ is satisfied for all values of R. For small ζ_i, the value of R must be large in order for the solution to be self-consistent. The present solution is now examined in the limit $\zeta - \zeta_i$ small and in the limit $R \to \infty$.

Consider $\zeta - \zeta_i$ small and $R \neq \infty$. The net power emitted up to station ζ is found by expanding I in a Taylor series about ζ_i and substituting into Eq. (29b). The result is

$$P(\zeta) = \bar{p}_0\Delta\nu_h G_c I_i(\zeta-\zeta_i)\left\{1 + O\left[\left(\frac{dI}{d\zeta}\right)_i(\zeta-\zeta_i)\right]\right\} \quad (46)$$

Thus, the output power is proportional to $\bar{p}_0\Delta\nu_h$ and is independent of R. In this case, particle residence time in the lasing region is too short for cross relaxation to contribute to the laser output.

In the limit $R \to \infty$, the solution becomes, for $j_f = 1$,

$$N_2 - N_1 = (N_2-N_1)_i + O(1/A) \quad (47a)$$

$$2(\bar{p}_0\Delta\nu_h)\zeta_D^{1/2}G_cI = \frac{2\pi p_1(\bar{p}_0\Delta\nu_h)}{1+\mathcal{L}(\Delta\nu_s/2)}$$

$$\times\left[\frac{1}{2\zeta_i^{1/2}} - \zeta_i^{1/2} - \zeta_D^{1/2}(N_2-N_1)_i\right] \quad \text{for } \zeta = \zeta_i \quad (47b)$$

$$= \frac{1}{2\zeta^{1/2}} - \zeta^{1/2} - \zeta_D^{1/2}(N_2-N_1)_i + O(e^{-A(\zeta-\zeta_i)})$$

$$+ O\left(\frac{1}{A}\right) \quad \text{for } \zeta > \zeta_i \quad (47c)$$

$$2\zeta_D^{1/2}P_e = \left[\zeta^{1/2} - \frac{2}{3}\zeta^{3/2} - \zeta_D^{1/2}(N_2-N_1)_i\zeta\right]_{\zeta_i}^{\zeta_e} + O\left(\frac{1}{A}\right) \quad (47d)$$

$$\zeta_e = \tfrac{1}{4}\left(\left\{[\zeta_D^{1/2}(N_2-N_1)_i)]^2 + 2\right\}^{1/2} - \zeta_D^{1/2}(N_2-N_1)_i\right)^2 \quad (47e)$$

In this limit the cross relaxation is sufficiently fast that the lasing medium acts like a homogeneous medium. There is no hole burning, and the results are the same as those deduced in Ref. 2. Note that I is discontinuous at $\zeta = \zeta_i$, a result of the assumption $R \to \infty$ and the corresponding neglect of the term of order $e^{-A(\zeta-\zeta_i)}$ in Eq. (47c).

Case $\Delta\nu_s \ll \Delta\nu_h$

Laminar cross flow solutions are obtained by the substitution of $N_T = (\zeta/\zeta_D)^{1/2}$ into Eqs. (40, 24b, and 29). Numerical integration is required.

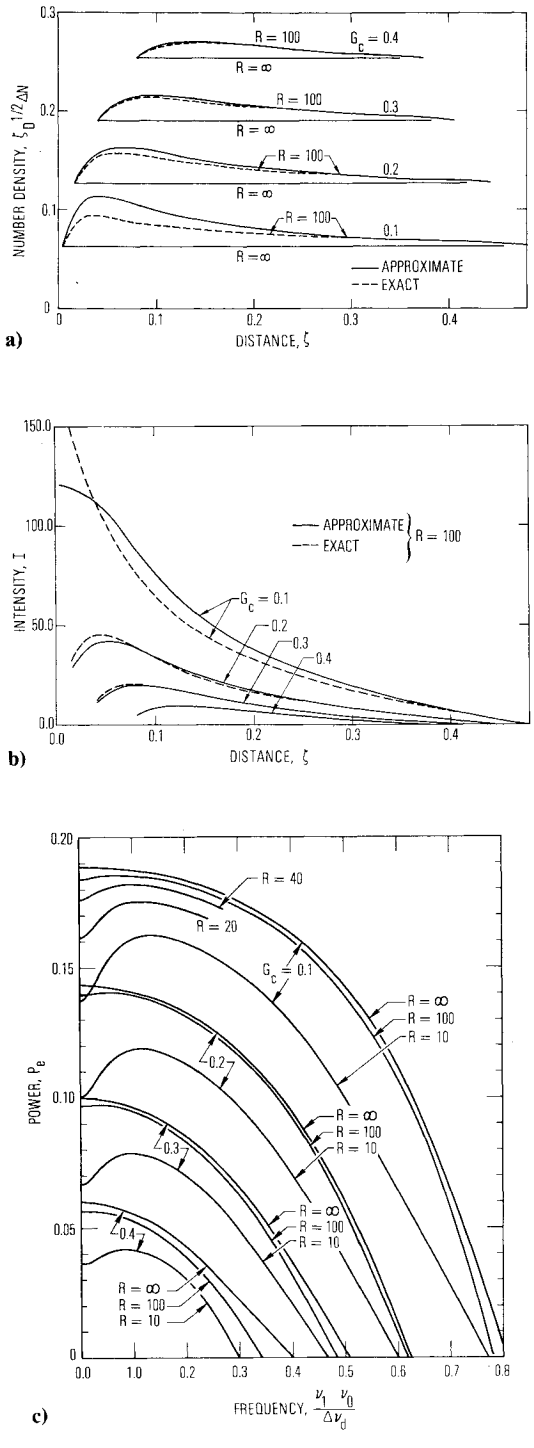

Fig. 5 Chemical laser performance for case of laminar mixing, single longitudinal model ($j_f = 1$), and $\Delta\nu_h/\Delta\nu_d = 0.1$. Equation (44) is used in approximate solution i.e., $[I/(1+R)]^2 \ll 1$. Equations (24b) and (40) are used in exact solution. a) $\zeta^{1/2}\Delta N$ vs ζ for $\nu_I = \nu_0$, $\zeta_i \le \zeta \le \zeta_e$; b) I vs ζ for $\nu_I = \nu_0$; c) P_e vs $(\nu_I - \nu_0)/\Delta\nu_d$.

III. Results and Discussion

The parameters deduced herein are similar to those in Ref. 2, except for the additional parameters $\bar{p}_0\Delta\nu_h = 0.9394\,\Delta\nu_h/\Delta\nu_d$ and R. Typical values for cw chemical lasers are discussed in Appendix A. In particular, $R = O$ (100) and $\Delta\nu_h/\Delta\nu_d = O[0.01 \times p(\text{Torr})]$, where p is the net static pressure in the lasing region and generally is in the range p (Torr) $= O$ (1-10). Since $\Delta\nu_h/\Delta\nu_d$ and R are small and large, respectively, in chemical lasers the latter generally appear as a product [e.g., Eqs. (34)] which can be approximated by $(\Delta\nu_h/$

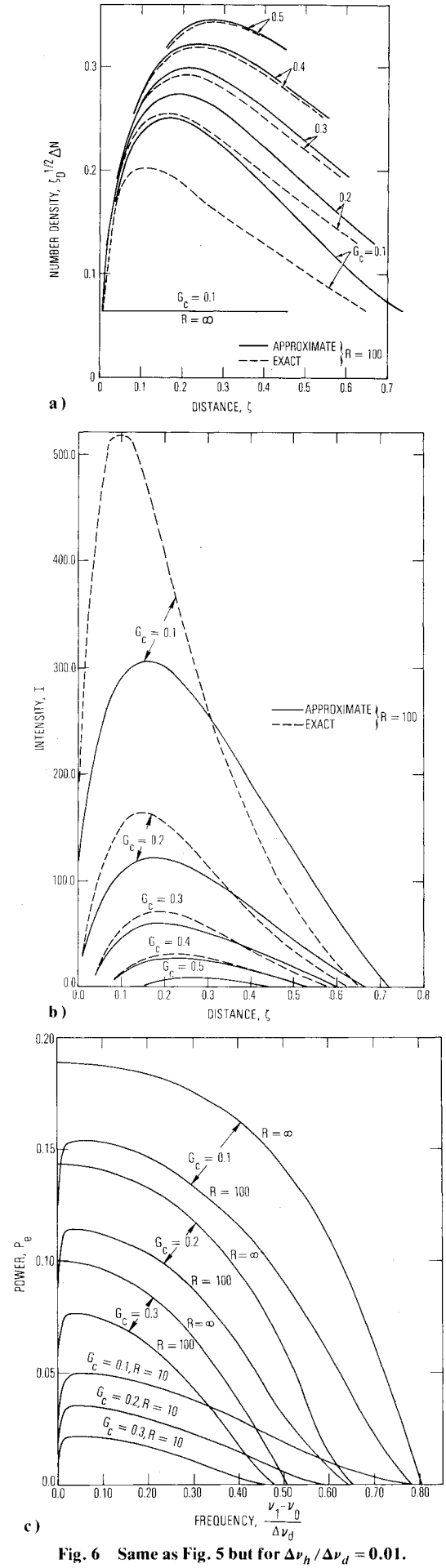

Fig. 6 Same as Fig. 5 but for $\Delta\nu_h/\Delta\nu_d = 0.01$.

Table 1 Chemical laser performance for case of laminar mixing, single longitudinal mode ($j_f = 1$), and $(\nu_l - \nu_0)/\Delta\nu_h = 0$

$\Delta\nu_h/\Delta\nu_d$	R	$\zeta_D^{1/2} G_c$	Exact [Eqs. (24b) and (40)] ζ_l	$\zeta_D^{1/2}\Delta N_l$	I_l	ζ_e	$\zeta_D^{1/2} P_e$	Approximate[a] [Eq. (44)] I_l	ζ_e	$\zeta_D^{1/2} P_e$	Asymptotic ($R\to\infty$) I_l	ζ_e	$\zeta_D^{1/2} P_e$
0.1	100	0.1	0.0041	0.0637	192.8	0.478	0.1856	120.7	0.481	0.1839	120.7	0.457	0.1887
		0.2	0.0170	0.1273	32.05	0.441	0.1400	28.13	0.442	0.1395	28.15	0.418	0.1433
		0.3	0.0407	0.1910	11.51	0.406	0.0970	10.92	0.406	0.0968	10.99	0.382	0.1000
		0.4	0.0808	0.2546	4.905	0.374	0.0562	4.791	0.374	0.0562	4.949	0.349	0.0600
		0.5	0.1566	0.3183	1.743	0.344	0.0183	1.726	0.344	0.0183	2.112	0.320	0.0257
	10	0.1	0.0041	0.0637	783.0	0.545	0.1736	120.7	0.635	0.1373			
		0.2	0.0170	0.1273	64.10	0.535	0.1171	28.13	0.579	0.1009			
		0.3	0.0407	0.1910	16.34	0.499	0.0741	10.92	0.521	0.0669			
		0.4	0.0808	0.2546	5.835	0.448	0.0386	4.791	0.457	0.0361			
		0.5	0.1566	0.3183	1.864	0.375	0.0104	1.726	0.377	0.0100			
0.01	100	0.1	0.0041	0.0637	192.8	0.639	0.1494	120.7	0.720	0.1239	120.7	0.457	0.1887
		0.2	0.0170	0.1273	32.05	0.626	0.1023	28.13	0.663	0.0905	28.15	0.418	0.1433
		0.3	0.0407	0.1910	11.51	0.585	0.0645	10.92	0.603	0.0594	10.99	0.382	0.1000
		0.4	0.0808	0.2546	4.905	0.528	0.0329	4.791	0.535	0.0312	4.949	0.349	0.0600
		0.5	0.1566	0.3183	1.743	0.442	0.0081	1.726	0.443	0.0079	2.112	0.320	0.0257
	10	0.1	0.0041	0.0637	783.0	0.815	0.0644	120.7	0.881	0.0282			
		0.2	0.0170	0.1273	64.10	0.756	0.0316	28.13	0.781	0.0197			
		0.3	0.0407	0.1910	16.34	0.667	0.0161	10.92	0.675	0.0122			
		0.4	0.0808	0.2546	5.835	0.557	0.0069	4.791	0.560	0.0060			
		0.5	0.1566	0.3183	1.846	0.418	0.0015	1.726	0.419	0.0014			

[a] $[I/(1+R)]^2 \ll 1$.

$\Delta\nu_d)R = O[p(\text{Torr})]$. As previously noted, inhomogeneous broadening effects become negligible in the limit $R\to\infty$. Effects of finite R can be deduced from the numerical results discussed subsequently.

Continuous-wave chemical laser performance has been evaluated for laminar mixing, a single longitudinal mode ($j_f = 1$), $0.1 \le G_c \le 0.5$, $0.01 \le \Delta\nu_h/\Delta\nu_d \le 0.1$, and $10 \le R \le 100$. The limit $R\to\infty$ has also been considered. The results are given in Table 1 and Figs. 5 and 6. Results for line-center operation, $\nu_l \to \nu_0$, are given in Table 1 and Figs. 5a, 5b, 6a, and 6b. The approximate theory, i.e., $[I/(1+R)]^2 \ll 1$, is in good agreement with the exact theory [Eqs. (24a) and 40)] for $[I_j/(1+R)]^2 \le O(1)$, particularly with regard to net output power P_e. The variation of the differential number density $\zeta_D^{1/2}\Delta N$ with ζ in the lasing region $\zeta_i \le \zeta \le \zeta_e$ is shown in Figs. 5a and 6a for $\Delta\nu_h/\Delta\nu_d = 0.1$ and 0.01, respectively. The quantity $\zeta_D^{1/2}\Delta N$ continues to increase, after lasing is initiated. The increase is more pronounced for $\Delta\nu_h/\Delta\nu_d = 0.01$. This result is in contrast with the homogeneous case ($R\to\infty$), where $\zeta_D^{1/2}\Delta N$ remains constant in the lasing region. Similarly, the local lasing intensity I tends to first increase with ζ and then decrease to zero (Figs. 5b and 6b). In the corresponding homogeneous medium, I decreases monotonically with ζ downstream of the region where lasing is initiated. The approximate theory tends to underestimate the upstream value of I and to overestimate the downstream values. Reasonably accurate estimates of net outpower P_e result even for those cases in which the approximate theory for the streamwise variation of I departs significantly from the exact theory. The effect on output power of operation off of line center is indicated in Figs. 5c and 6c. For $R \ne \infty$, the output power has local minimum at $\nu_l = \nu_0$ because $I^+(\nu_0)$ and $I^-(\nu_0)$ compete for the same molecules. The output power first increases with an increase in ν_l since $I^+(\nu_l)$ and $I^-(\nu_l)$ tend to interact with different molecules. The power is at maximum at $\nu_l - \nu_0 = O(\Delta\nu_h)$. Thereafter, P_e decreases with increase in ν_l because of the decrease in $p(\nu)$. The resultant dip is similar to that deduced by Lamb.[6] For a given value of G_c, the departure from the curves $R = \infty$ in Figs. 5c and 6c represents the effect of inhomogeneous broadening on output power. The departure is small when $(\Delta\nu_h/\Delta\nu_d)R \ge 10$. Thus, the departure should be small when cw chemical lasers operate in the pressure regime $p(\text{Torr}) \ge O(10)$. Inhomogeneous broadening effects become important for single-mode lasers operating in the regime $p(\text{Torr}) \le O(1)$. In this pressure regime, however, the use of multiple longitudinal modes [i.e., $\Delta\nu_c/\Delta\nu_d \ll 1$ and $\Delta\nu_h/\Delta\nu_c = O(1)$] can result in efficient power extraction.

The Lamb dip has been observed, experimentally, in cw chemical lasers. The variation of single mode output power with lasing frequency[4] is reproduced in Fig. 7 and is similar to the curves in Figs. 5c and 6c.

The streamwise variation of index of refraction can also be determined. Consider cases wherein there is no mode competition, i.e., $\Delta\nu_s \gg \Delta\nu_h$. The index of refraction at each lasing transition ν_j can be expressed (e.g., as Eqs. (28), (29c), and Appendix B).

$$\frac{(2\pi/\lambda)[\eta(\nu_j) - I]}{g_c} = \frac{\phi_j D(X)}{\pi^{1/2} p_j}[I + O(Y)] \qquad (48)$$

where X, Y, and ϕ_j are defined in Appendix B and g_c is the threshold gain [Eq. (15)]. Equation (48) is similar in form to the result deduced from Lamb's theory[6,10] wherein $\phi_j g_c/p_j$ represents line center-zero power gain. The local value of index of refraction in the present model is seen to depend on ϕ_j, which is a measure of the local degree of saturation and is evaluated from the solution of Eqs. (24b) and (28). For cases where $(\Delta\nu_h/\Delta\nu_d)R \gg 1$, Eq. (47c) indicates that $\phi_j = 1 + 0\{[(\Delta\nu_h/\Delta\nu_d)R]^{-1}\}$. For the latter cases, "hole-burning" effects are negligible since the local index of refraction equals the value for an inhomogeneously broadened medium with

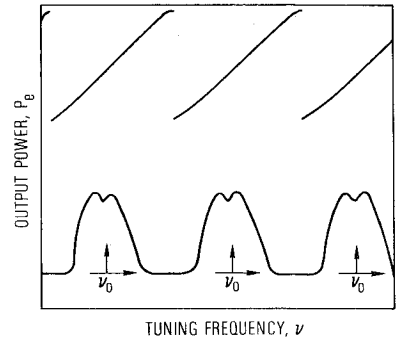

Fig. 7 Single-mode power tuning curves for the $P_2(4)$ laser transition of HF. Experimental results are from Ref. 4.

line center gain equal to g_c/p_j. That is, the index of refraction is proportional to the threshold gain and is unaffected by the zero power gain.

IV. Concluding Remarks

It has been assumed that the streamwise length of the Fabry-Perot resonator equals the streamwise length of the positive gain region in order to extract as much power as possible from the lasing medium. In these cases ζ_e is of order one (e.g., Table 1) and the resonator length x_e is of the order of the characteristic collisional deactivation distance $x_{cd}=u/k_{cd}$. Thus, the particle transient time x_e/u is of the order of the characteristic collisional deactivation time k_{cd}^{-1}. The result that inhomogeneous broadening effects are small for $(\Delta\nu_h/\Delta\nu_d)R \geq O(10)$ is therefore physically realistic since $\Delta\nu_h/\Delta\nu_d$ is a measure of the fraction of the excited particles which are resonant with the laser radiation field and R is a measure of the number of times the resonant and nonresonant excited particles are interchanged by cross relaxation during transit through the resonator. Parameter values in the range $(\Delta\nu_h/\Delta\nu_d)R > 1$ imply that all excited particles are resonant with the laser radiation field at some time during transit through the resonator.

Inhomogeneous broadening effects become more severe in low-pressure cw chemical lasers when the streamwise length of the resonator is smaller than the streamwise length of the positive gain region. In the latter case, the number of particle collisions per transit through the resonator is of order $(\Delta x_c/x_{cd})R$, where Δx_c is the resonator length, and inhomogeneous broadening effects are expected to be negligible when

$$(\Delta x_c/x_{cd})(\Delta\nu_h/\Delta\nu_d)R \geq O(10) \tag{49}$$

The latter reduces to the previous expression $(\Delta\nu_h/\Delta\nu_d)R \geq O(10)$ when the resonator length is of the order of the streamwise length of the positive gain region (i.e., when Δx_c is of order x_{cd}). Equation (49) may be viewed as a generalized criteria which accounts for arbitrary resonator length. The influence of resonator length on inhomogeneous effects in cw chemical lasers has been observed experimentally. In particular, longitudinal mode pulling[1] was found to be more severe when a stable resonator ($\Delta x_c \doteq 0.1$ cm) was applied to a cw chemical laser supersonic gain medium ($x_{cd} \doteq 1$ cm)[14] than when an unstable resonator ($\Delta x_c \doteq 1$ cm) was applied.[15]

Appendix A: Characteristic Values of Parameters

Characteristic values of line shape parameters, rate parameters, and stimulated emission coefficients are given herein with emphasis on HF lasers.

A. Line Shape

Doppler Broadening

The characteristic width of a Doppler-broadened line shape is (FWHM)

$$\Delta\nu_d = 7.163\times10^{-7}\nu_0(T/M)^{1/2}\ (\mathrm{s}^{-1}) \tag{A1}$$

where T is in K, and M is the molecular weight of the lasing molecule in grams per mole. For an HF laser ($M=20$, $\lambda = 2.77\times10^{-6}$ m), $\Delta\nu_d = 300\times10^6(T/300)^{1/2}$.

Pressure Broadening

The characteristic width of a pressure-broadened line shape can be expressed[3,16] (FWHM) as

$$\Delta\nu_h = 5.996\times10^{10}\sum_i p_i(\mathrm{atm})\gamma_i(\mathrm{atm}^{-1}\ \mathrm{cm}^{-1})\ (\mathrm{s}^{-1}) \tag{A2}$$

where p_i is the partial pressure of species i and γ_i is the broadening coefficient for that species. The coefficient γ_i depends on temperature level, as well as rotational and vibrational energy levels J and v, respectively. Values of γ_i are given in Table 2 for HF and DF lasing molecules perturbed by various other molecules. For a typical hard sphere collision,[8] $\gamma_i = k_{gk}/(2\pi c p_i)$ [Eq. (A7)]. Typical partial pressures in a cw HF chemical laser[14] are $p_i/p = 0.12$, 0.39, 0.47, and 0.02 for species n_i = HF, He, H_2, and O_2, respectively. With room temperature values of the broadening coefficients, i.e., $\gamma_i = 0.2$, 0.005, 0.03 and 0.03, respectively, it is found that $\Delta\nu_h/300\times10^6 = 0.01\ p(\mathrm{Torr})$, where p(Torr) is the net static pressure in Torr in the lasing region. It follows that under typical cw HF laser operating conditions

$$\frac{\Delta\nu_h}{\Delta\nu_d} = 0.01p(\mathrm{Torr}) \tag{A3}$$

Generally, $p(\mathrm{Torr}) = O(10)$, and $\Delta\nu_h/\Delta\nu_d = O(0.1)$.

B. Rates

Reactions of the form

$$A + B \xrightarrow{\bar{k}} C + D \tag{A4a}$$

$$\frac{\mathrm{d}[A]}{\mathrm{d}t} = -\bar{k}[B][A] \equiv -k[A] \tag{A4b}$$

are of concern, where $k \equiv \bar{k}[B]$ is an average rate coefficient. (Note that k^{-1} is the characteristic time for the reaction.) An average value of $[B]$ is used in the definition of k. The latter is in units of s^{-1} and can be expressed in the form

$$\frac{k}{p_B} = \frac{\bar{k}[B]}{p_B} = \frac{\bar{k}}{\Re T} \tag{A4c}$$

where $\Re$ is the universal gas constant.

Collisional Deactivation Rate

From Ref. 12, the HF collisional deactivation process is characterized by the rate for the process

$$\mathrm{HF}(v) + \mathrm{HF} \xrightarrow{\bar{k}_{cd}} \mathrm{HF}(v-1) + \mathrm{HF} \tag{A5a}$$

$$\frac{\mathrm{d}[\mathrm{HF}(v)]}{\mathrm{d}t} = -k_{cd}[\mathrm{HF}(v)] \tag{A5b}$$

where[12]

$$\frac{k_{cd}}{p_{\mathrm{HF}}} = \frac{v}{82.06T}\left(\frac{3\times10^{14}}{T} + 3.5\times10^4 T^{2.26}\right) \tag{A6}$$

The choice $v = 2$ provides a typical value for k_{cd}.

Hard-Sphere Collision Rate

Let k_{gk} deote the number of collisions per unit time that a particle of species A undergoes with the particles of species B. The quantity $(k_{gk})^{-1}$ is the characteristic time between collisions. For a hard sphere model,

$$\frac{k_{gk}}{p_B} = \frac{8.40\times10^{25}}{\phi}\frac{(\sigma_A+\sigma_B)^2}{T^{1/2}}\left(\frac{1}{M_A}+\frac{1}{M_B}\right)^{1/2}(\mathrm{s}^{-1}\ \mathrm{atm}^{-1}) \tag{A7}$$

where k_{gk} is termed the "gas kinetic" collision rate. Here, $\phi = 1$ and 2 are for $A = B$ and $A \neq B$, respectively, and σ is the particle diameter in centimeters. The gas kinetic rate for collisions between an HF molecule and other HF molecules is

Table 2 *P*-branch $(v+1, J-1 \rightarrow v, J)$ pressure-broadening coefficients

Temperature, K	Rotational level, J	Coefficient γ_i, $cm^{-1}\ atm^{-1}$	Molecules Lasing	Molecules Perturbing	Reference
373	$6 \le J \le 10$	0.25 -0.09	HF	HF	3
400	$6 \le J \le 10$	0.15 -0.08	HF	DF	3
400	$6 \le J \le 10$	0.36 -0.20	DF	HF	3
400	$6 \le J \le 10$	0.40 -0.18	DF	DF	3
373	$5 \le J \le 8$	0.030-0.020	HF	H_2	3
373	$6 \le J \le 8$	0.034-0.024	HF	N_2	3
300	$J \ge 1$	0.005	HF	He	16
300	$6 \le J \le 8$	0.005-0.015	HF	Ar	16

Table 3 Cross relaxation rate $R = k_{cr}/k_{cd}$ for HF based on Eqs. (A7) and (A5) with $v = 2$

Temperature T,K	100	200	300	400	500	600	700	800	900	1000
R	10.6	29.8	54.3	81.8	110.3	137.4	160.8	178.8	190.8	196.6

(note that $\sigma_{HF} = 2.7 \times 10^{-8}$ cm, and $\phi = 1$)

$$\frac{k_{gk}}{p_{HF}} = 4.47 \times 10^9 \left(\frac{300}{T}\right)^{1/2} (s^{-1}\ atm^{-1}) \tag{A8}$$

Collisions of HF with other species are not considered herein. It can be assumed that the number density distribution function $n(v)$ is randomized after each collision between HF and a particle of similar or greater mass. Hence, assume $k_{cr} = k_{gk}$. Corresponding values of R, for an HF laser, are given in Table 3. It is seen that $10 < R < 200$ for $100 < T < 1000$. Despite the supersonic expansion in cw chemical lasers, the temperature in the lasing region tends to be of order 500 K because of reaction heating and nozzle wall boundary layer effects. Thus, typically, $R = O(100)$.

Stimulated Emission Coefficients

The gain for a *P*-branch transition $(v+1, J-1 \rightarrow v, J)$ can be written for the case of rotational equilibrium,

$$g_{v,J} = \sigma_{v,J}\,(n_{v+1} - e^{-2JT_R/T} n_v) \tag{A9}$$

An approximate expression for the line center value of $\sigma_{v,J}$ for an HF laser is[12] (with $\Delta\nu_h \ll \Delta\nu_d$ assumed)

$$\sigma_{v,J} = \frac{4.26 \times 10^{11}}{T^{3/2}} \frac{(1+v-0.01v^3)(1+0.063J)J}{\exp[J(J-1)T_R/T]} \left(\frac{cm^2}{mol}\right) \tag{A10}$$

where $T_R = 30.16$ K. Comparison with the present development indicates

$$\sigma_0 \tilde{p}_0 \Delta\nu_h = (2/\pi)\sigma_{v,J} \tag{A11}$$

As previously noted, $\sigma_0 \Delta\nu_h$ is independent of pressure.

Appendix B: Mathematical Expressions

The mathematical expressions given here have been used in the present study. Integrals involving the Lorentzian line shape have the form

$$\int_{-\infty}^{\infty} \mathcal{L}(\nu' - \nu) \frac{d\nu}{\Delta\nu_h} = \frac{\pi}{2} \tag{B1a}$$

$$\int_{-\infty}^{\infty} [\mathcal{L}(\nu' - \nu)]^2 \frac{d\nu}{\Delta\nu_h} = \frac{\pi}{4} \tag{B1b}$$

$$\int_{-\infty}^{\infty} \mathcal{L}(\nu' - \nu)\mathcal{L}(\nu'' - \nu) \frac{d\nu}{\Delta\nu_h} = \frac{\pi/4}{1 + [(\nu'' - \nu')^2/(\Delta\nu_h)^2]} \tag{B1c}$$

$$\frac{2}{\pi} \int_{-\infty}^{\infty} \frac{p(\nu)\mathcal{L}(\nu_j - \nu)\,d\nu/\Delta\nu_h}{1 + [2I_j/(1+R)]\mathcal{L}(\nu_j - \nu)} = \frac{1}{\phi_j}\left\{e^{-X^2} - \frac{2}{\sqrt{\pi}} Y[1 - 2XD(X)] + O(Y^2)\right\} \tag{B1d}$$

$$\frac{4}{\pi} \int_{-\infty}^{\infty} \frac{\nu_j - \nu}{\Delta\nu_h} \frac{p(\nu)\mathcal{L}(\nu_j - \nu)\,d\nu/\Delta\nu_h}{1 + [2I_j/(1+R)]\mathcal{L}(\nu_j - \nu)} = \frac{2}{\sqrt{\pi}} D(X) - 2XYe^{-X^2} + O(Y^2) \tag{B1e}$$

where

$$\phi_j = \left(1 + \frac{2I_j}{1+R}\right)^{1/2}$$

$$X = 2\sqrt{\ell n 2}\,(\nu_j - \nu_0)/\Delta\nu_d$$

$$Y = \sqrt{\ell n 2}\,(\Delta\nu_h/\Delta\nu_d)\phi_j$$

and $D(X)$ is the Dawson integral which has the following properties:

$$D(z) = e^{-z^2} \int_0^z e^{z_0^2} dz_0 \tag{B2a}$$

$$= z\left[1 - \frac{2}{3}z^2 + \frac{4}{15}z^4 + \ldots\right] \tag{B2b}$$

$$= \frac{1}{2z}\left[1 + \frac{1}{2z^2} + \frac{3}{4z^4} + \ldots\right] \tag{B2c}$$

$$\frac{1}{A}\frac{dD[(A\zeta)^{1/2}]}{d\zeta} = \frac{1}{2(A\zeta)^{1/2}} - D[(A\zeta)^{1/2}] \tag{B3a}$$

$$A\int_0^{\zeta} D[(A\zeta_0)^{1/2}]\,d\zeta_0 = (A\zeta)^{1/2} - D[(A\zeta)^{1/2}] \tag{B3b}$$

Acknowledgment

This work reflects research supported by the Defense Advanced Research Projects Agency under U.S. Air Force Space and Missile Systems Organization (SAMSO) Contract No. F04701-77-C-0078.

References

[1] Bennett, W. R., Jr., "Hole Burning Effects in a He-Ne Optical Maser," *Physical Review*, Vol. 126, April 1961, pp. 580-593.

[2] Mirels, H., Hofland, R., and King, W. S., "Simplified Model of CW Diffusion Type Chemical Laser," *AIAA Journal*, Vol. 11, Feb. 1973, pp. 156-164.

[3] Emanuel, G., "Numerical Modeling of Chemical Lasers," *Handbook of Chemical Lasers*, edited by R.W.F. Gross and J. F. Bott, John Wiley and Sons, New York, 1976, pp. 488-496.

[4] Glaze, J. A., "Linewidth Parameters from the Lamb Dip in a CW Chemical Laser," *Applied Physics Letters*, Vol. 23, Sept. 1973, pp. 300-302.

[5] Spencer, D. J., Beggs, J. A., and Mirels, H., "Small-Scale CW HF (DF) Chemical Laser," *Journal of Applied Physics*, Vol. 48, March 1977, pp. 1206-1211.

[6] Sargent, M., III, Scully, M. O. and Lamb, W. R., Jr., *Laser Physics*, Addison-Wesley Publishing Co., Reading, Mass., 1974, pp. 144-155.

[7] Kan, T. and Wolga, G. J., "Influence of Collisions on Radiative Saturation and Lamb Dip Formation in CO_2 Molecular Lasers," *IEEE Journal Quantum Electronics*, Vol. QE 7, April 1971, pp. 141-150.

[8] Maitland, A. and Dunn, M. H., *Laser Physics*, Wiley, New York, 1969, pp. 42-54 and 384-387.

[9] Abramowitz, M. and Stegun, I. A., *Handbook of Mathematical Functions*, AMS 55, National Bureau of Standards, U.S. Government Printing Office, Washington, D.C., June 1964, pp. 297-303.

[10] Close, D. H., "Strong-Field Saturation Effects in Laser Media," *Physical Review*, Vol. 153, Jan. 1967, pp. 360-371.

[11] Cabezas, A. Y. and Treat, R. P., "Effect of Hole Burning and Cross Relaxation on the Gain Saturation of Laser Amplifiers," *Journal of Applied Physics*, Vol. 37, Aug. 1966, pp. 3556-3563.

[12] Mirels, H., "Simplified Model of a CW Diffusion-Type Chemical Laser-An Extension," *AIAA Journal*, Vol. 14, July 1976, pp. 930-939.

[13] Broadwell, J. E., "Effect of Mixing Rate on HF Chemical Laser Performance," *Applied Optics*, Vol. 13, April 1974, pp. 962-967.

[14] Spencer, D. J., Mirels, H., and Durran, D. A., "Performance of a CW HF Chemical Laser with N_2 or He Diluent," *Journal of Applied Physics*, Vol. 43, March 1972, pp. 1151-1157.

[15] Chodzko, R. A. and Wang, C. P., Private communication, The Aerospace Corporation, El Segundo, Calif., Dec. 1977.

[16] Hough, J.J.T., "Lorentz Broadening in the Modeling of the HF Chemical Laser," *Applied Optics*, Vol. 16, Aug. 1977, pp. 2297-2307.